Catalysis Today 140 (2009) 30–36

Contents lists available at ScienceDirect

Catalysis Today

journal homepage: www.elsevier.com/locate/cattod

Epimerisation of menthol stereoisomers: Kinetic studies of the heterogeneously catalysed menthol production

B. Etzold [a], A. Jess [a,*], M. Nobis [b,1]

[a] Department of Chemical Engineering, University of Bayreuth, D-95447 Bayreuth, Germany
[b] Symrise AG, D-37603 Holzminden, Germany

ARTICLE INFO

Article history:
Available online 9 September 2008

Keywords:
Menthol
Menthone
Epimerisation
Synthetic menthol

ABSTRACT

The heterogeneously catalysed epimerisation of neomenthol and isomenthol is a key step in the synthesis of menthol in the Symrise process (formerly know as Haarmann & Reimer process). A reaction model based on the experimentally determined kinetic and thermodynamic parameters was derived for industrial relevant conditions of 150–210 °C and 0.8–7.5 MPa hydrogen pressure. Results of experiments and modelling show a good agreement and thus the derived kinetic parameters can be used for the optimisation of batch slurry processes as well as of continuous fixed bed processes.

1. Introduction

The terpene alcohol (−)-menthol is after vanilla and citrus the most important flavouring substance and is used in toothpastes, preshave lotions and many other cosmetic products [1]. (−)-Menthol has a unique cooling effect and flavour. Besides flavouring (−)-menthol is also used in pharmacy and medicine because of its anastatic properties (e.g. for contact urticaria, treatment of headache or acute bronchitis) [1–6]. Another field is the tobacco industry where around 25% of the menthol production is used.

Worldwide, about 18,000 tonnes of (−)-menthol are produced per year (2006) [7]. The majority is natural menthol from mentha arvensis or mentha piperita and only around 1/4 are produced synthetically. Nevertheless, the synthetic route is important. The price of (−)-menthol from natural resources fluctuates strongly if the availability is limited due to bad harvests. Thus the synthetically produced (−)-menthol based on different feedstocks stabilises the price [8–10].

Stereochemical aspects have to be taken into account for the synthetic production of (−)-menthol. The core of menthol is a non-planar cyclohexane ring which has a methyl, hydroxyl and a isopropyl substitute. From the two common conformations of cyclohexane – the chair and the boat form – the chair form is thermodynamically preferred. The substituting groups can stay in axial or equatorial position [2,11,12].

Menthol has three chiral centers, thus eight different conformers are possible. These are (+)- and (−)-menthol, (+)- and (−)-neomenthol, (+)- and (−)-isomenthol and (+)- and (−)-neoisomenthol (Fig. 1). Due to the already mentioned properties of (−)-menthol, where all substitutes are in the equatorial position, this isomer is the by far most desired product.

In general, two routes are used for the industrial synthesis of (−)-menthol. One option is to achieve a chiral precursor very early in the process and hold up the chiral information during the whole process to gain only the (−)-menthol in the end. This is done in the Takasago-process in Japan.

Alternatively, a racemic mixture of (±)-menthol can be synthesised by the heterogeneously catalysed hydrogenation of thymol, followed by a separation of the target molecule (−)-menthol by distillation and crystallisation. This is done in the Symrise process (formerly know as Haarmann & Reimer process), as shown in Fig. 2 [2,8,13–16].

The hydrogenation of thymol leads to an equilibrium of racemic mixtures of about 60% of (±)-menthol, 30% of (±)-neomenthol and 10% of (±)-isomenthol. (±)-Neoisomenthol is formed in a negligible amount [1]. Thus 40% of undesired stereoisomers have to be separated by distillation and are subsequently catalytically converted on a Ni-catalyst by epimerisation. The resulting menthol-rich mixture is recycled into the distillation.

In this work, the epimerisation of the menthol stereoisomers as a center part of the process was studied.

The epimerisation is carried out with a nickel catalyst under hydrogen pressure (5–10 MPa) at temperatures of 150–200 °C in a trickle bed reactor with very long residence times.

* Corresponding author at: Lehrstuhl für Chemische Verfahrenstechnik, Universität Bayreuth, Universitätsstrasse 30, D-95440 Bayreuth, Germany.
Tel.: +49 921 557430; fax: +49 921 557435.
E-mail address: Jess@uni-bayreuth.de (A. Jess).
[1] Present address: IO3S, CH-3014 Bern, Switzerland.

0920-5861/$ – see front matter © 2008 Elsevier B.V. All rights reserved.
doi:10.1016/j.cattod.2008.07.009

Nomenclature

c	concentration (mol m^{-3})
c_{cat}	catalyst concentration (kg m^{-3})
$E_{A,i}$	activation energy of reaction i (J mol^{-1})
$\Delta_R H^\circ$	reaction enthalpy (J mol^{-1})
iso	isomenthol
$k_{0,i}$	pre-exponential factor for reaction i (m^3 kg^{-1} s^{-1})
k_i'	rate constant of reaction i (m^3 kg^{-1} s^{-1})
K	equilibrium constant
m	menthol
neo	neomenthol
p_{H_2}	hydrogen pressure (MPa)
r	reaction rate (mol kg^{-1} s^{-1})
R	gas constant (8.314 J mol^{-1} K^{-1})
$\Delta_R S^\circ$	reaction entropy (J mol^{-1} K^{-1})
T	temperature (K)
x	mole fraction (mol%)

Greek symbols

ρ	density (kg m^{-3})
τ	modified residence time (kg s m^{-3})

Although hydrogen is formally not needed according to the stoichiometry of the epimerisation, it is needed to suppress the unwanted dehydrogenation to menthon (see Fig. 5).

2. Experimental and data analysis

A commercial lab-scale semibatch reactor with a magnetic stirrer (Büchi Limbo 350) was used for the kinetic experiments. The catalyst (typically around 4 g) is filled in a basket fixed inside the autoclave and activated at 300 °C under hydrogen. Afterwards the reactant mixture (typically 150 ml; ≈50 mol% (±)-neomenthol, ≈25 mol% (±)-menthol, ≈25 mol% (±)-isomenthol, ≈1 mol% menthone) is filled into the autoclave. The reactant mixtures and the catalyst were supplied by Symrise. The hydrogen pressure was kept constant during the reaction. The speed of the magnetic stirrer and the temperature inside the autoclave are controlled. Samples are taken through a dip pipe and analysed by means of a gas chromatograph (Varian 3800/FID, CP-Chirasil-DEX CB 25 m × 0.25 mm, 50–135 °C with 3 °C/min). Neoisomenthol cannot be detected, but fortunately it is unimportant for the kinetic description as its concentration changes only from 3 mol% (feed) to 1.5 mol% (final value for long residence times) and thus influences the concentration profile only to a negligible extend [17].

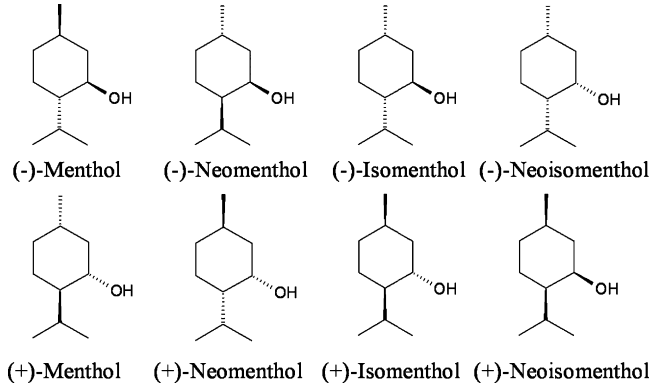

Fig. 1. Structure of the eight menthol diastereomers.

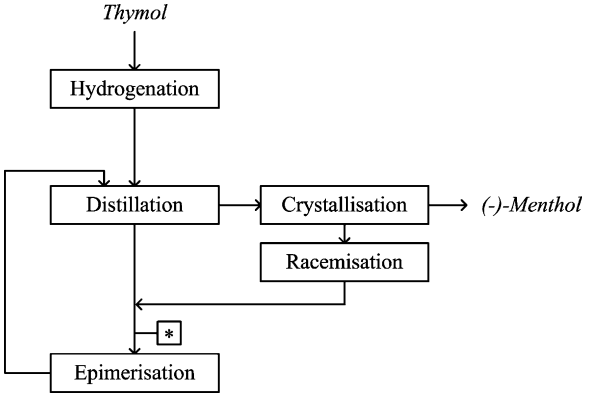

Fig. 2. Simplified flow sheet of the Symrise process for menthol production; *: reactant mixture for the studies.

In this work the concentrations of the conformers are summed up to a pseudo-component, as it has been proven that all enantiomers react with the same velocity and the reaction orders of the stereoisomers are one (see Section 3.3). Thus, the reaction model developed in this work only considers the reaction rates of the three racemic mixtures of menthol, neomenthol, and isomenthol. If in this paper a stereoisomer is named without (+) or (−) notation, the racemic mixture is always meant.

Three differential equations with 10 parameters are needed to describe the reaction network, i.e. the change of the concentrations of menthol, neomenthol and isomenthol (see Section 3.6). These equations were solved numerically by the computer program Presto Kinetics (CiT GmbH, Rastede, Germany, version 3.16.1). The same software was used for the parameter estimation where the least squares objective function of absolute values is minimized by the Damped Gauss–Newton-algorithm. As a measure for the reaction time which does not depend on the concentration of the catalyst c_{cat}, the modified residence time is used throughout this work, defined as the actual reaction time in the batch reactor used for the kinetic studies multiplied with the concentration of the catalyst c_{cat}.

3. Results and discussion

3.1. Catalyst stability and catalyst activation

The catalyst consists mainly of nickel oxide. It is activated by reduction with hydrogen. The optimum temperature for the reduction of the catalyst was unknown at the beginning of the study. Activation experiments at different temperatures showed that a temperature above 200 °C is sufficient to activate the catalyst completely. At temperatures above 300 °C the catalyst looses activity by sintering. This was determined by BET analysis after tempering the catalyst in air for 10 h. Fig. 3 clearly shows that a strong decrease of the internal surface area starts at around 350 °C. Thus a reduction temperature of 300 °C was chosen for an optimal catalyst activation. The kinetic experiments and temperature programmed reduction studies showed that the activation of the catalyst is fast and that a standard reduction time of 1.5 h is sufficient (for details see [18]).

3.2. Mass transport limitations

Prior to the study of the intrinsic kinetics, the influence of any external and internal mass transfer limitations was excluded.

To determine the influence of mass transport, experiments with different particle sizes, stirring speeds and catalyst concentrations were done. The experiments with small particle sizes (<500 μm) were carried out with a suspended catalyst. For larger particles, the

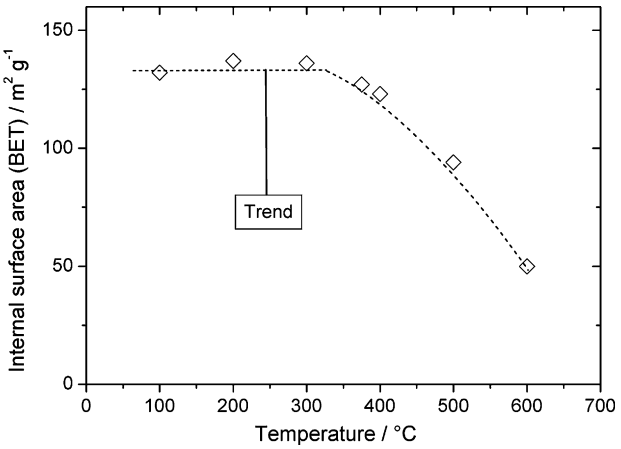

Fig. 3. Decrease of internal (BET) surface area due to sintering (tempering in a muffle kiln for 10 h under air at each temperature).

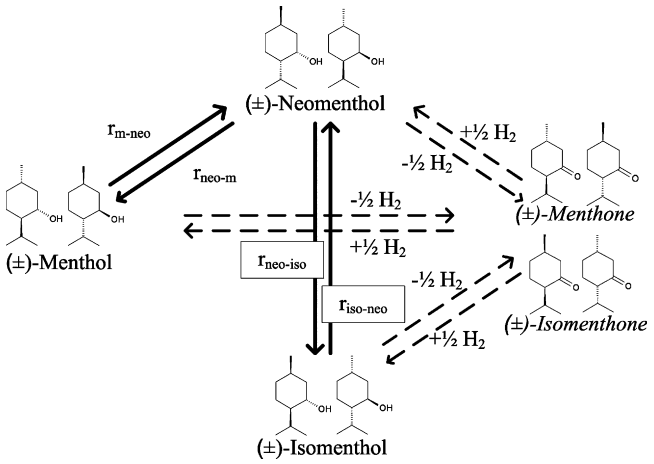

Fig. 5. Reaction scheme used to derive the differential equations (without side reaction to menthone) of the kinetic model for the epimerisation of menthol diastereomers.

catalyst was fixed in a basket which was mounted inside the batch slurry phase reactor.

Since hydrogen is not consumed during the epimerisation, no limitation of the gas–liquid mass transport was expected, but nevertheless proven. Indeed, the variation of the stirring speed and catalyst concentration showed no effect on the observed reaction rates and a limitation of the gas–liquid mass transport can be excluded [18]. The variation of the particle size from 63 to 1000 μm also showed no effect and thus no liquid–solid or internal mass transfer limitations (pore diffusion) have to be considered. So for the given reaction conditions, the intrinsic chemical kinetics were measured in the lab-scale batch reactor.

3.3. Intrinsic chemical kinetics

Fig. 4 shows a typical concentration–residence time plot for the epimerisation of the menthol stereoisomers. The results calculated by the kinetic model are also already given. The neomenthol of the feed (~50%) reacts relatively fast to menthol while isomenthol reacts slowly. The conversion to menthol is limited by thermodynamic constraints, e.g. for the conditions given in Fig. 4 only about 58% of menthol are finally formed. Thus the kinetics of the forward and backward reactions are needed to model the system.

For an accurate kinetic description based on not too many kinetic parameters it was necessary to simplify the complex reaction network to an reaction scheme (shown in Fig. 5) [18]. An undesired reaction that may also play a role is the dehydrogenation to menthone [19,20]. Fortunately, for a hydrogen pressure above 1.5 MPa the menthone concentration is below 2 mol% (at 185 °C) and thus the reactions leading to menthone (dashed arrows in Fig. 5) can then be neglected in the model.

Mechanism which are discussed in literature for the epimerisation of menthol stereoisomers always include an reaction at the hydroxyl group. There an intermediate could be a Δ^2- or Δ^3-enolate or a Meerwein–Ponndorf–Verley reduction with a menthone stereoisomer or an dehydrogenation to menthone followed by a keto-enol-tautomerism and hydrogenation could take place [20–23]. This could be verified in this work by epimerising pure (−)-menthol as feedstock, which gave only (+)-neomenthol and (+)-isomenthol as products. As a reaction from (+)-isomenthol to (+)-menthol could not be observed even at long reaction times, an epimerisation at the methyl group can be excluded. This result leads to four reversible reactions which have to be taken into account ((−)-menthol ↔ (+)-neomenthol ↔ (+)-isomenthol, (+)-menthol ↔ (−)-neomenthol ↔ (−)-isomenthol). As expected no change in the ratios of (+) to (−) stereoisomers occurred during the epimerising of the industrial racemic feed-

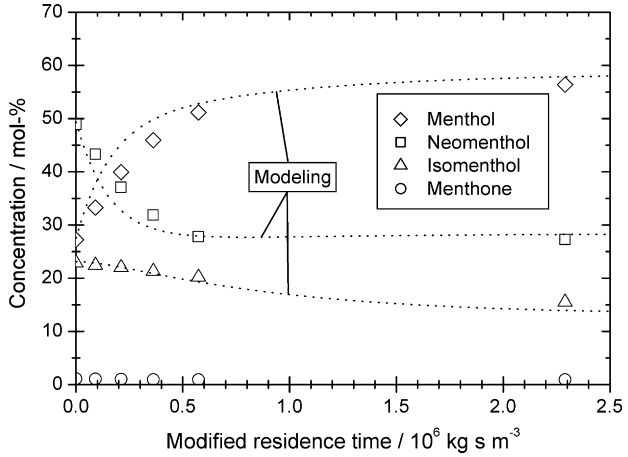

Fig. 4. Typical experimental result of the kinetic studies of the epimerisation of menthol diastereomers (standard reactant mixture, 185 °C; $p_{H_2} = 7.5$ MPa).

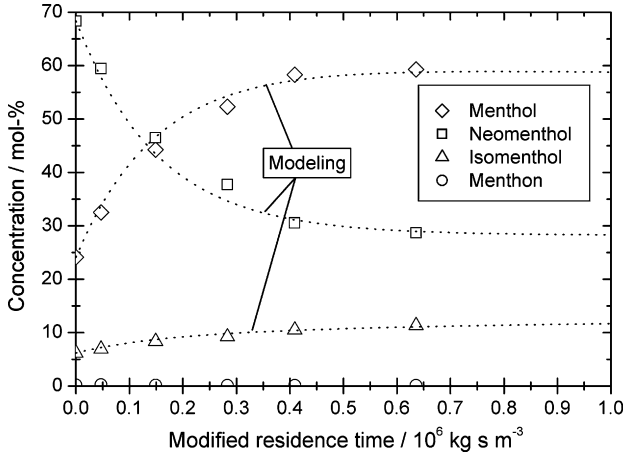

Fig. 6. Kinetic experiment with a neomenthol-rich feed as reactant mixture to determine the reaction orders (185 °C; $p_{H_2} = 7.5$ MPa).

stock and only racemic mixtures have to be taken into account. This reduces the reaction network to two reversible reactions ((±)-menthol ↔ (±)-neomenthol ↔ (±)-isomenthol, Fig. 5). The experiments showed that all reactions are first order with respect to the menthol stereoisomers. This was deduced and proven by comparison of the calculated and measured concentration–residence time plots for different feed mixtures. Besides the standard (industrial relevant) feed mixture with 50 mol% (±)-neomenthol and 25 mol% both of (±)-menthol and (±)-isomenthol, a neomenthol-rich (~90 mol% neomenthol) as well as an isomenthol-rich (~55 mol% isomenthol) mixture was also used. Fig. 4 (standard mixture) and Fig. 6 (neomenthol-rich feed) show the good agreement of the model with the experimental data, which is also true for a isomenthol-rich feed [18].

The reactions are limited by the thermodynamical equilibrium and thus the knowledge of the until now unknown equilibrium concentrations and of the deduced equilibrium constants is needed to model the reaction system. For example, the equation for the formation of neomenthol is given by (see Fig. 5):

$$\frac{dc_{neo}}{d\tau} = r_{m-neo} - r_{neo-m} + r_{iso-neo} - r_{neo-iso} \quad (1)$$

At first, the experiments were carried out under a constant hydrogen pressure and thus the reaction-rate constants were described by a pseudo-reaction-rate constant k' which incorporates the influence of the concentration of the dissolved hydrogen and thus of the hydrogen pressure. The individual reaction rates are

$$r_{neo-m} = k'_{neo-m} c_{neo} \quad (2)$$

$$r_{m-neo} = k'_{m-neo} c_m = \frac{k'_{neo-m}}{K_{neo-m}} c_m \quad \text{with } K_{neo-m} = \frac{c^*_m}{c^*_{neo}} \quad (3)$$

$$r_{iso-neo} = k'_{iso-neo} c_{iso} \quad (4)$$

$$r_{neo-iso} = k'_{neo-iso} c_m = \frac{k_{iso-neo}}{K_{iso-neo}} c_m \quad \text{with } K_{iso-neo} = \frac{c^*_{neo}}{c^*_{iso}} \quad (5)$$

So the two reversible reactions of menthol formation can be described by the rate constants of the forward reactions and the two equilibrium constants. The respective differential equations for the change of the concentrations of neomenthol and isomenthol are derived in the same way and are not explicitly given here (see [18]).

The equilibrium concentrations c^* were determined based on experiments at different temperatures and hydrogen pressures (although the latter should not have and had not any influence) to calculate the equilibrium constants. The equilibrium constants are given by

$$K_i = \exp\left(\frac{-\Delta_R H_i^\circ}{RT} + \frac{\Delta_R S_i^\circ}{R}\right) \quad (6)$$

and the up to now unknown values of $\Delta_R H_i^\circ$ and $\Delta_R S_i^\circ$ of the two equilibrium constants were calculated based on the best fit with the experimental values at different temperatures (Table 1). By Eq. (6) the equilibrium constants can be calculated as a function of the temperature. Assuming that only menthol, neomenthol and isomenthol are present, the equilibrium concentration can be solved by a mass balance. For example, the molar equilibrium content of the main product menthol is given by

$$x_{menthol} = \frac{1}{1 + (1/K_{neo-m}) + (1/K_{neo-m}K_{iso-neo})} \quad (7)$$

Literature values of the equilibrium concentrations and own measured data are compared with the calculated values in Fig. 7. The agreement of the calculation with the experimental data over a wide range of temperature is very satisfactory.

Table 1
Equilibrium constants for the epimerisation of menthol diastereomers

T (°C)	K_{neo-m}	$K_{iso-neo}$
150	2.3	2.3
175	2.1	2.2
200	2.0	2.1
225	1.9	2.0

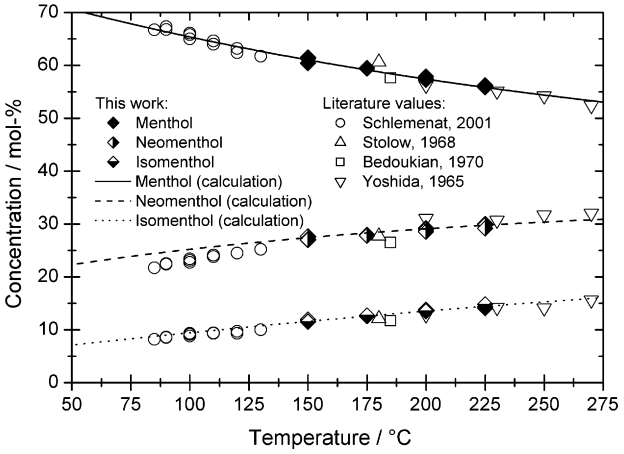

Fig. 7. Equilibrium concentrations of the menthol diastereomers over the temperature. Comparison of measured (150–250 °C), calculated and literature values (70–270 °C) [19,26–28].

3.4. Influence of hydrogen pressure

Two problems arise with the description of the kinetics with regard to hydrogen: (1) Hydrogen is not consumed during the epimerisation, but nevertheless influences the epimerisation rates and thus has to be considered for the kinetic modelling. (2) For low hydrogen pressures, menthone formation cannot be neglected.

Initially, the influence of the hydrogen pressure was incorporated into the global first-order rate constants k'_i. The assumption of constant k'_i values (for a given hydrogen pressure) is acceptable,

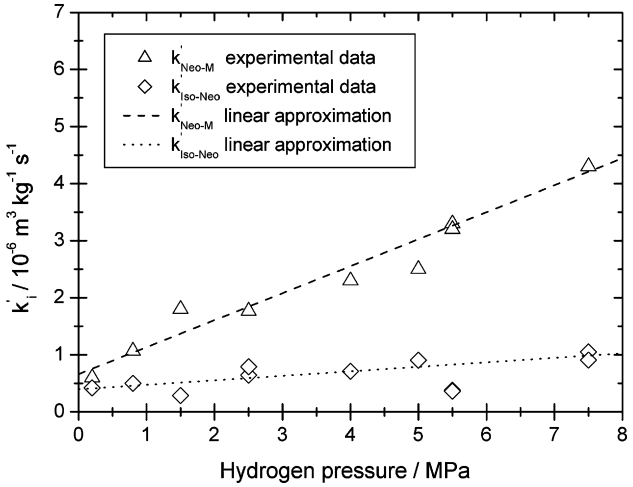

Fig. 8. Influence of hydrogen pressure on k'_i (values estimated with the software Presto from experiments at different hydrogen pressures at 185 °C).

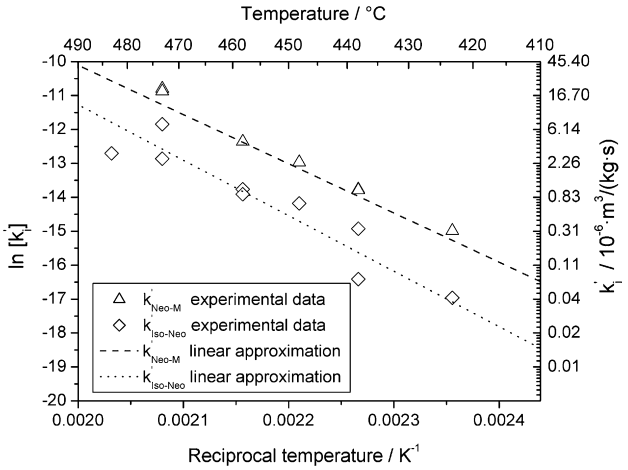

Fig. 9. Influence of temperature on k_i' (values estimated with the software Presto from experiments at different temperatures at $p_{H_2} = 7.5$ MPa).

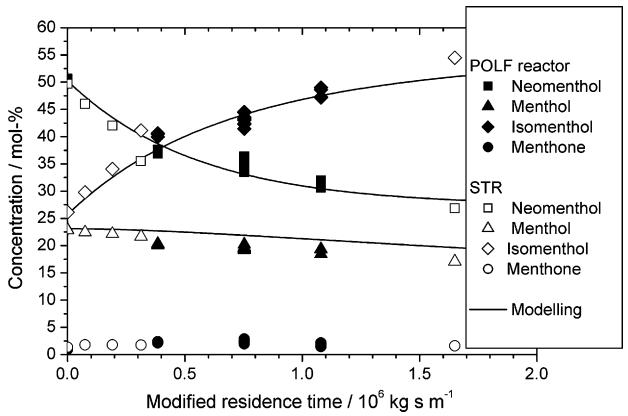

Fig. 10. Experimental results of the POLF reactor at 180 °C, $p_{H_2} = 2$ MPa, d_{kat} = 250–500 μm, m_{kat} = 70 g compared with the modelling and results of the semibatch reactor.

as the hydrogen pressure and hence the concentration of the dissolved hydrogen are constant in the semibatch reactor used.

The influence of the hydrogen pressure on the reaction rates was studied by varying the hydrogen pressure from 0 (experiment with nitrogen) to 7.5 MPa (pure H_2) at 185 °C. With increasing hydrogen pressure the unwanted dehydrogenation is strongly suppressed. For example, for a hydrogen pressure of 2.5 MPa less than 1.5% (at 185 °C) of menthone are formed (the feed mixture already had about 1% menthone). Thus a lower pressure should be avoided. The dehydrogenation to menthone is favoured by high temperatures, and thus temperatures above 200 °C should also be avoided.

Fig. 8 clearly indicates that the rate constants k' are a function of the hydrogen pressure. The rate constants show a linear trend, and without hydrogen the reaction comes not to a complete standstill.

The reason is probably that the menthol stereoisomers are at first adsorbed under hydrogen scission on the catalyst surface. Thus, for the consecutive epimerisation reaction (adsorbed) hydrogen is needed which may explain the higher rates with elevated hydrogen pressure (at least for the given conditions). This behaviour is depicted in Fig. 8. Anyway, the influence of pressure on the rate constants at 185 °C can be formally described by the following equations:

$$k'_{\mathrm{neo-m}}\,(185\,^{\circ}\mathrm{C}) = 5.08 \times 10^{-13}\,\mathrm{kg\,s^{-1}\,m^{-3}\,Pa^{-1}}\,(1.04 \times 10^{6}\,\mathrm{Pa} + p_{H_2}) \quad (8)$$

$$k_{\mathrm{iso-neo}}\,(185\,^{\circ}\mathrm{C}) = 9.48 \times 10^{-14}\,\mathrm{kg\,s^{-1}\,m^{-3}\,Pa^{-1}}\,(4.02 \times 10^{6}\,\mathrm{Pa} + p_{H_2}) \quad (9)$$

where the first term represents the "real" rate constant k_i that only depends on temperature (for the reaction model, it was assumed that the influence of pressure as described by Eqs. (8) and (9) does not depend on temperature).

Table 2
Kinetic and thermodynamic parameters of the reaction

Parameter	Value	Relative standard error (%)
$k_{0,\mathrm{neo-m}}$	750 $m^3\,kg^{-1}\,s^{-1}\,Pa^{-1}$	1.93
$E_{A,\mathrm{neo-m}}$	133 kJ mol^{-1}	0.05
$p_{0,\mathrm{neo-m}}$	1.04×10^6 Pa	6.71
$k_{0,\mathrm{iso-neo}}$	1.20×10^4 $m^3\,kg^{-1}\,s^{-1}\,Pa^{-1}$	3.31
$E_{A,\mathrm{iso-n}}$	150 kJ mol^{-1}	0.09
$p_{0,\mathrm{iso-neo}}$	4.02×10^6 Pa	7.95
$\Delta_R H^{\circ}_{\mathrm{neo-m}}$	−4.03 kJ mol^{-1}	0.84
$\Delta_R S^{\circ}_{\mathrm{neo-m}}$	−2.79 J $mol^{-1}\,K^{-1}$	2.68
$\Delta_R H^{\circ}_{\mathrm{iso-neo}}$	−3.23 kJ mol^{-1}	1.38
$\Delta_R S^{\circ}_{\mathrm{iso-neo}}$	−0.406 J $mol^{-1}\,K^{-1}$	2.18

3.5. Influence of temperature

To determine the influence of temperature, experiments were carried out from 150 to 210 °C at 7.5 MPa hydrogen pressure. Based on the Arrhenius correlation for k_i' we get

$$k_i' = k_i\,f(p_{H_2}) = k_{0,i}\,e^{(-(E_{A,i}/RT))}(p_{0,i} + p_{H_2}) \quad (10)$$

and

$$\ln(k_i') = \ln(k_i^0) + \ln(p_{0,i} + p_{H_2}) - \frac{E_{A,i}}{R}\,\frac{1}{T} \quad (11)$$

For a hydrogen pressure of 7.5 MPa, the plot of $\ln(k_i')$ vs. $1/T$ gives a straight line (Fig. 9). The activation energy is calculated from the slope E_A/R. The reaction of neomenthol to menthol and reverse is much faster than the other reactions (see Fig. 8). Therefore $k'_{\mathrm{neo-m}}$ has a greater influence on the calculated results than $k'_{\mathrm{iso-neo}}$. This can be seen at the statistical output of the parameter estimation. There the value of the 95% confidence interval (3.8% for $k'_{\mathrm{neo-m}}$ and 6.5% for $k'_{\mathrm{iso-neo}}$) represents the sensitivity of the parameter variation on the calculated result. Thus $k'_{\mathrm{iso-neo}}$ can be varied in a larger interval without influencing the calculated results, which leads to a more inexact estimation of the parameter. This is the

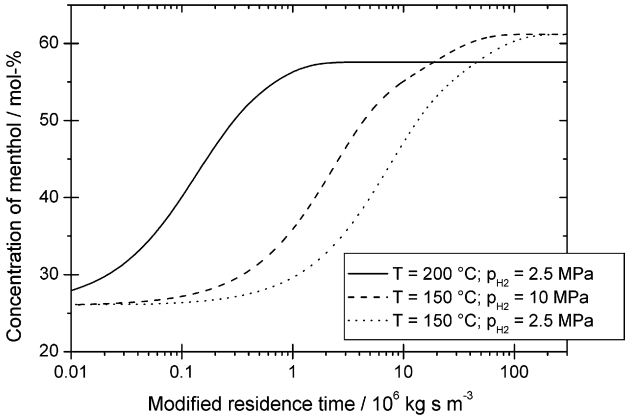

Fig. 11. Modelling of concentrations vs. modified residence time (intrinsic kinetic) for an temperature and hydrogen pressure variation.

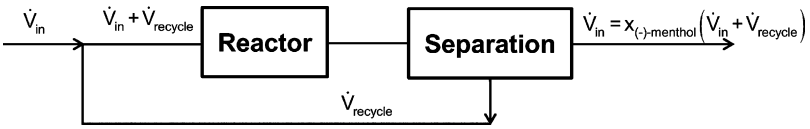

Fig. 12. Scheme to derive the minimum recycle rate in the Symrise process when (−)-menthol is the only product and perfect separation is assumed.

reason why the parameter estimation values for $k'_{iso-neo}$ disperse more in Figs. 8 and 9.

3.6. Combined temperature and pressure influence

All parameters for the combined description of the influence of temperature and pressure on the kinetics and on the equilibrium were derived in the previous sections. Because the solubility of hydrogen in the liquid reaction phase changes only to minor extend with the temperature compared to the reaction rate, it was assumed that the separation of the pressure and temperature dependencies like in Eq. (10) can be done. Thus $k_{0,i}$ as the only missing parameter can be calculated. The parameters $p_{0,i}$ and E_A are known and the last missing parameter $k_{0,i}$ can be calculated using Eq. (10). Thus the final form of the differential equations describing the change of the concentrations of all components can be derived, using the reaction scheme in Fig. 5:

$$-\frac{dc_M}{d\tau} = [k_{0,neo-M}(p_{H_2} + p_{0,neo-M})\, e^{(-(E_{A,neo-M}/RT))}] [e^{((\Delta_R H^\circ_{neo-M}/RT)-(\Delta_R S^\circ_{neo-M}/R))} c_M - c_{neo}] \quad (12)$$

$$-\frac{dc_{neo}}{d\tau} = [k_{0,neo-M}(p_{H_2} + p_{0,neo-M})\, e^{(-(E_{A,neo-M}/RT))}] [c_{neo} - e^{((\Delta_R H^\circ_{neo-M}/RT)-(\Delta_R S^\circ_{neo-M}/R))} c_M] + [k_{0,iso-neo}(p_{H_2} + p_{0,iso-neo})\, e^{(-(E_{A,iso-neo}/RT))}] [e^{((\Delta_R H^\circ_{iso-neo}/RT)-(\Delta_R S^\circ_{iso-neo}/R))} c_{neo} - c_{iso}] \quad (13)$$

$$-\frac{dc_{iso}}{d\tau} = [k_{0,iso-neo}(p_{H_2} + p_{0,iso-neo})\, e^{(-(E_{A,iso-neo}/RT))}][c_{iso} - e^{((\Delta_R H^\circ_{iso-neo}/RT)-(\Delta_R S^\circ_{iso-neo}/R))} c_{neo}] \quad (14)$$

The solution of the differential equations and the numerical fit of the parameters was done by the computer programme already mentioned in Section 2.

The model parameters are summarised in Table 2 and are valid in a range of 0.8–7.5 MPa hydrogen pressure and 150–210 °C. The overall residual between the calculation and the measured data results to 0.059.

3.7. Validation on a POLF reactor

The obtained kinetic data were validated by a continuous presaturated one-liquid flow (POLF) reactor. In the POLF reactor the liquid is saturated with gas in a pre-saturator outside the reactor as described in more detail in [24,25]. Hence, only the saturated liquid is fed into a fixed bed reactor. The advantage is that only two phases, the liquid saturated with hydrogen and the solid catalyst are present inside the reactor. In case of epimerisation, hydrogen is anyway only needed to suppress the dehydrogenation and is thus not consumed. Consequently, the concentration of the dissolved hydrogen does not change in the fixed bed and there is no need for the delivery of fresh H_2. To validate the kinetic data experimental results of the POLF reactor, the semibatch reactor and the modelling are compared in Fig. 10. The results show a good agreement.

A second experiment to validate the kinetic data was made in the semibatch reactor. There a temperature (195 °C) and hydrogen pressure (3 MPa) was chosen, which was not used to obtain kinetic data. The results are not shown here but also agree very fine with the modelling [18].

3.8. Simulation of operation conditions

The influence of the temperature and hydrogen pressure on the residence time to reach 99% of the equilibrium concentration of menthol was finally simulated with the kinetic data. For the simulation isothermal operation was assumed as the reaction enthalpy of the epimerisation is only very small ($\Delta_R H \approx -4$ kJ/mol) and thus a rise in temperature is negligible. Mass transfer limitations were also neglected which may have an influence depending on the used reactor and catalyst size. The influence of mass transfer limitations is examined in more detail in [18] and will be the subject of subsequent publications. Fig. 11 shows the simulated concentrations vs. the modified residence time.

At 150 °C the hydrogen pressure was varied in the simulation from 2.5 to 10 MPa (Fig. 11). The modified residence time to reach 99% of the equilibrium concentration of menthol decreases from 1.1×10^8 to 4.6×10^7 kg s m^{-3}. Thus an increase of the hydrogen pressure is advantageous and in addition the dehydrogenation to the unwanted by-product menthone is suppressed.

Increasing the temperature from 150 to 200 °C (at 2.5 MPa) also decreases the modified residence time to reach 99% of the equilibrium concentration of menthol (1.3×10^6 kg s m^{-3}). As the epimerisation is slightly exothermic this improvement in the reaction rate decreases the equilibrium concentration of the product menthol. At 150 °C 61 mol% of menthol can be obtained and at 200 °C only 57 mol%. This affects not only the product quality but also the whole process as the by-products are recycled. Assuming that the equilibrium concentration is reached and that despite (−)-menthol everything is recycled, a minimum recycle rate can be calculated. From the mass balance (Fig. 12) the minimum recycle rate as a function of the mole fraction of (−)-menthol is given by

$$\varphi = \frac{V_{recycle}}{V_{in}} = \frac{1}{x_{(-)\text{-menthol}}} - 1 \quad (15)$$

Taking the equilibrium concentrations for the mole fraction of (−)-menthol at 150 °C a minimum recycle rate of 2.28 and at 200 °C of 2.48 results.

Thus the increase of the temperature has not only a positive effect on the reaction rate but also the negative effect of lowering the menthol yield, which results in a higher recycle rate.

4. Conclusions

An intrinsic kinetic model for the reaction network of the epimerisation of menthol stereoisomers was developed based on the experimentally determined kinetic and thermodynamic parameters.

The reaction rates strongly increase with temperature but the equilibrium concentration of the target compound menthol then also slightly decreases.

The formation of the unwanted byproduct menthon can be suppressed by hydrogen. Although hydrogen is not consumed by

the epimerisation, the reaction rates increase almost linearly for an increase of the hydrogen pressure from 1.5 to 7.5 MPa.

The agreement of the experimental and modelled data shows that the derived kinetic parameters can be used for the design and optimisation of slurry phase batch reactors as well as of continuous fixed bed processes. Based on this result the influence of mass transfer will be studied in subsequent works.

References

[1] R. Emberger, R. Hopp, Speciality Chem. Mag. 7 (1987) 193–201.
[2] G.T. Walker, Manuf. Chemist Aerosol News 38 (1967) 51–53.
[3] J. Scavroni, C.S.F. Boaro, M.O.M. Marques, L.C. Ferreira, Braz. J. Plant Physiol. 17 (2005) 345–352.
[4] H. Bast, DRAGOCO-Berichte (1956) 136–139.
[5] N. Ravasio, F. Zaccheria, A. Fusi, R. Psaro, Appl. Catal. A: Gen. 315 (2006) 114–119.
[6] A.F. Trasarti, A.J. Marchi, C.R. Apesteguia, J. Catal. 247 (2007) 155–165.
[7] G.S. Clark, Perfumer Flavorist 32 (2007) 38–47.
[8] G.S.I.V. Clark, Perfumer Flavorist 23 (1998) 33–46.
[9] S.C. Varshney, Perfumer Flavorist 30 (2005) 36ff.
[10] H. Surburg, J. Panten, Common Fragrance and Flavor Materials Preparation, Properties and Uses, Wiley–VCH, Weinheim, 2006.
[11] S. Mignat, F. Porsch, Dragoco Rept. 8 (1961) 232–244.
[12] E.L. Eliel, Experientia 9 (1953) 91–93.
[13] J.C. Leffingwell, R.E. Shackelford, Cosmet. Perfumery 89 (1974) 69–78.
[14] B.M. Lawrence, Mint: The Genus Mentha, CRC Press, Boca Raton, 2007.
[15] J. Read, W.J. Grubb, J. Soc. Chem. Ind. Lond. 51 (1932) 323–329.
[16] R. Hopp, Riv. Ital. EPPOS 7 (1996) 111–130.
[17] I.-L. Gatfield, E.-M. Hilmer, U. Bornscheuer, R. Schmidt, S. Vorlova, EP 1223223 (2002).
[18] B. Etzold, Epimerisierung der Menthol-Stereoisomere: Kinetische und reaktionstechnische Studien für die heterogen katalysierte Mentholsynthese, PhD thesis, University of Bayreuth, Shaker Verlag, Aachen, 2008.
[19] T. Yoshida, A. Komatsu, M. Indo, Agric. Biol. Chem. 29 (1965) 824–831.
[20] S. Mignat, F. Porsch, Dragoco Rept. 8 (1961) 267–279.
[21] W.v.E. Doering, T.C. Aschner, J. Am. Chem. Soc. 71 (1949) 838–840.
[22] W. Hückel, C.Z.K. Cheema, Chem. Ber. 91 (1958) 311–319.
[23] H. Rothbaecher, F. Suteu, A. Kraus, J. Prakt. Chem. 36 (1967) 153–159.
[24] S. Peter, L. Datsevich, A. Jess, Appl. Catal. A: Gen. 286 (2005) 96–110.
[25] S. Peter, Reaktionskinetik und Reaktionstechnik der Hydrierung von Feinchemikalien in Mehrphasenreaktoren, PhD thesis, University of Bayreuth, Germany, 2005.
[26] A. Schlemenat, R. Langer, C. Dreisbach, H.-J. Gross, T. Prinz, A. Schulze-Tilling, M. Friederich, J.D. Jentsch, G. John, DE 10023283 (2001).
[27] R.D. Stolow, T. Groom, Tetrahedron Lett. (1968) 4069–4072.
[28] P.Z. Bedoukian, Am. Perfumer Cosmet. 85 (1970) 25–35.